ELSEVIER

Biochimica et Biophysica Acta 1364 (1998) 373–384

BIOCHIMICA ET BIOPHYSICA ACTA
BBA

Kinetics of electron and proton transfer to ubiquinone-10 and from ubiquinol-10 in a self-assembled phosphatidylcholine monolayer

Maria Rosa Moncelli, Roberto Herrero, Lucia Becucci, Rolando Guidelli *

Chemistry Department, University of Florence, Via G. Capponi, 9, 50121-Florence, Italy

Received 2 February 1998; accepted 5 March 1998

Abstract

Upon incorporating from 0.5 to 2 mol% ubiquinone-10 (UQ) in a self-assembled monolayer of dioleoylphosphatidylcholine (DOPC) supported by mercury, the kinetics of UQ reduction to ubiquinol-10 (UQH_2) as well as that of UQH_2 oxidation to UQ were investigated in borate buffers over the pH range from 8 to 9.5 by cyclic voltammetry. A general kinetic approach was adopted to interpret the dependence of the applied potential upon the scan rate at constant pH and upon pH at constant scan rate, while keeping the initial reactant concentration and the faradaic charge constant. The oxidation of UQH_2 to UQ in DOPC monolayers occurs via the reversible release of one electron with formation of the semiubiquinone radical cation $UQH_2^{\cdot +}$, followed by its rate-determining deprotonation by hydroxyl ions with formation of the $UQH^{\cdot}$ neutral radical; the latter is then instantaneously oxidized to UQ. Analogously, the rate-determining step in UQ reduction to UQH_2 consists in the protonation by hydrogen ions of the semiubiquinone radical anion $UQ^{\cdot -}$ resulting from the reversible uptake of one electron by UQ. However, a non-negligible fraction of $UQ^{\cdot -}$ uptakes protons very slowly, and hence, retains its intermediate oxidation state during the recording of the cyclic voltammetric peak for UQ reduction.

Keywords: Ubiquinone-10; Ubiquinol-10; Phosphatidylcholine monolayer

1. Introduction

Ubiquinone-10 (UQ) is an integral component of the respiratory chain that mediates the electron transfer in the inner mitochondrial membrane and participates in the translocation of protons across the membrane. In spite of the intense activity aiming at elucidating the mechanism of its function, details of the reduction mechanism of UQ and of the oxidation mechanism of ubiquinol-10 (UQH_2) in membranes remain somewhat controversial. The mechanistic features of the UQ/UQH_2 transformation are rather complex, since the overall two-electron, two-proton transfer may proceed through several different pathways, depending on the nature of the environment. Results obtained from aprotic solvent studies [1–3] can hardly be transposed to the membrane case where, although UQ and UQH_2 are present in a lipidic environment, water and its dissociation products may well participate in intermediate chemical steps. Recently, various self-assembly procedures have been devised to incorporate UQ in lipid layers supported by metal electrodes and in contact with aqueous solutions, with the aim of simulating the membrane environment. Thus, the electrochemical behaviour of

* Corresponding author.

0005-2728/98/$19.00
PII S0005-2728(98)00061-9

UQ has been investigated at a *n*-alkanethiol modified gold electrode [4], within a phospholipid layer deposited on a *n*-alkanethiol modified gold electrode [5], within a thick phospholipidic matrix added on a pyrolytic graphite electrode [6] and in a supported phospholipid bilayer obtained by vesicle fusion [7]. The use of membrane models to investigate UQ behaviour is of significant interest since the location of UQ within phospholipid membranes [8] and its lateral mobility are critical to its function [5]. Naturally, the reaction pathway of the UQ/UQH_2 system in biomembranes may also be significantly affected by the binding of the polar functional quinone group to redox-active proteins [9], an aspect beyond the scope of the present work.

The mechanism of electroreduction of UQ incorporated in a self-assembled monolayer of phosphatidylcholine (PC) deposited on mercury was recently investigated in this laboratory [10]. The lipid coating was provided by spreading a solution of the lipid in pentane on the surface of an aqueous electrolyte, allowing the solvent to evaporate, and immersing a hanging mercury drop electrode in the electrolyte [11–15]. Over the potential range from -0.2 to -0.8 V(SCE), these lipid monolayers are impermeable to inorganic ions and behave like half-membranes, with the polar heads directed towards the aqueous solution [11]. Thus, the differential capacity of phospholipid films supported by mercury ranges from 1.6 to 1.8 μF cm^{-2} depending on the nature of the lipid and of the aqueous electrolyte, and hence, is about twice as high as that of planar bilayer lipid membranes (BLMs). These lipid monolayers are highly reproducible, completely solvent-free and exhibit a high mechanical stability.

A quantitative analysis of the mechanism by which important mitochondrial redox components of the electron-transport chain such as UQ and ubiquinol, UQH_2, undergo electron and proton transfer while being incorporated in a self-assembled, defect-free lipid monolayer in contact with an aqueous solution is of significance from a biophysical viewpoint since it simulates biologically relevant conditions. In Moncelli et al. [10], the investigation of UQ reduction on phosphatidylcholine-coated mercury electrodes was carried out by a computerized chronocoulometric apparatus [16], which makes use of a very fast operational amplifier for current integration. This apparatus is particularly suitable for recording fast transients, but the stability of the operational amplifier does not allow a sufficiently accurate integration of the very low currents (of the order of 1 pA) that flow after $0.5 \div 1$ s from the instant of a potential jump. Hence, our chronocoulometric apparatus could not be used to investigate the reverse process of UQH_2 oxidation to UQ. In fact, at the most positive potentials at which the lipid monolayer still behaves like a half-membrane, complete oxidation of UQH_2 to UQ requires a few seconds. The present work aims at investigating the mechanism of UQH_2 oxidation to UQ as a function of pH by cyclic voltammetry (CV), using potential scan rates low enough to follow the corresponding kinetics. The investigation of UQ reduction to UQH_2 by long time-scale cyclic voltammetry confirms substantially the mechanistic conclusions drawn from chronocoulometric measurements [10], but reveals some further interesting features. Thus, it points out that a non-negligible fraction of the intermediate semiubiquinone radical anion $UQ^{\cdot -}$ uptakes protons very slowly, and hence, retains its intermediate oxidation state during the recording of the whole cyclic voltammetric peak for UQ reduction.

2. Experimental

The adsorbed monolayers of dioleoylphosphatidylcholine (DOPC) on mercury were prepared as described earlier [11–13]. The water used was obtained by distilling light mineral water, and by then distilling the water so-obtained from alkaline permanganate. Merck reagent grade KCl was baked at 500°C before use to remove any organic impurities. DOPC from Lipid Products (South Nutfield, Surrey, England) and horse-heart ubiquinone-10 (UQ) from Sigma were used without further purification. Working solutions of lipid and UQ in pentane for spreading at the air–water interface were prepared everyday and stored at -20°C. All measurements were carried out in aqueous 0.1 M KCl at 25°C. The pH was controlled with a $HBO_2/NaBO_2$ buffer from 8.5 to 9.5. The overall concentration of the acidic and basic components of the buffer is referred to as the buffer concentration.

The home-made hanging mercury drop electrode (HMDE) employed in the measurements, the cell and

the detailed procedure to produce self-assembled lipid monolayers deposited on mercury are described elsewhere [12–14]. All potentials were measured vs. a saturated calomel electrode (SCE). Differential capacity measurements were carried out using a Metrohm Polarecord E506 (Herisau, Switzerland). Cyclic voltammograms were recorded with an Amel Mod. 473 Polarographic Analyzer (Milano, Italy). Each cyclic voltammogram was recorded on a newly formed lipid-coated mercury drop.

Before the recording of cyclic voltammograms, the differential capacity C of the lipid monolayer was always measured against the applied potential E to check the stability and reproducibility of the film. The C vs. E curves obtained with UQ concentrations ≤ 0.5 mol% in the DOPC monolayer practically coincide with those obtained with pure DOPC; in particular, the differential capacity along the flat minimum in the C vs. E curves assumes the same value of about 1.75 μF cm^{-2} for both cases. With an increase in the UQ concentration, a single immersion of the mercury drop through the layer of (DOPC + UQ) spread on the solution surface was usually found not to be sufficient to attain the same differential capacity minimum as that of a pure DOPC monolayer. To achieve this goal, an increasing number of successive immersions of the same mercury drop was normally required. Further electrochemical measurements were carried out only after attaining this result. At UQ concentrations, > 2 mol% experimental measurements became progressively more irreproducible even upon adopting the above-procedure.

The charge density σ_M on the lipid-coated mercury drop at constant applied potential was measured by using a variant of the lipid-coated mercury electrode [17] suggested by the pioneering work by Miller [18]. Briefly, the surface of the lipid-coated electrode was contracted by an accurately measured amount while keeping its neck in contact with the (DOPC + UQ) layer previously spread on the surface of the aqueous solution; under these conditions, the lipid monolayer supported by mercury remains in equilibrium with the 'lipid reservoir' and hence, retains its properties upon contraction. The charge flowing along the external circuit as a consequence of this contraction, once divided by the decrease in the drop area, provides a measure of the charge density σ_M on the mercury surface, with an accuracy of 0.02 μC cm^{-2}.

3. Results

Fig. 1 shows a typical cyclic voltammogram obtained from a DOPC monolayer containing 1.5 mol% UQ in contact with a pH 9.5 buffer solution of 0.1 M KCl by scanning the potential from -0.1 to -0.7 V(SCE) and vice versa at a scan rate of 5 mV/s. The peak for UQ reduction and that for UQH_2 oxidation are both well-developed. A gradual increase in the scan rate causes a negative shift in the reduction peak and a positive shift in the oxidation one, with a resulting increase in the separation between the two peaks. The potential, E_{mp}, of the midpoint between the potential, $E_{r,p}$, of the maximum of the reduction peak and the potential, $E_{o,p}$, of the maximum of the oxidation peak is not affected by the scan rate. A gradual increase in pH causes a negative shift of both the reduction and the oxidation peaks. Thus, the midpoint potential E_{mp} shifts by about 60 mV in the negative direction per each unitary increment in pH, as shown in Fig. 2. Over the whole pH range investigated, a change in the buffer concentration from 5×10^{-4} to 5×10^{-2} M at constant pH has no appreciable effect on the reduction and oxidation peaks. The midpoint potential E_{mp} in Fig. 2 can be taken as a measure of the formal potential of the UQ/UQH_2 couple in the DOPC monolayer. It is interesting to observe that this formal potential and its pH dependence practically coincide with those determined by Gordillo and Schiffrin [19] from the cyclic voltammograms of UQ submonolayers deposited on mercury by a procedure consisting in

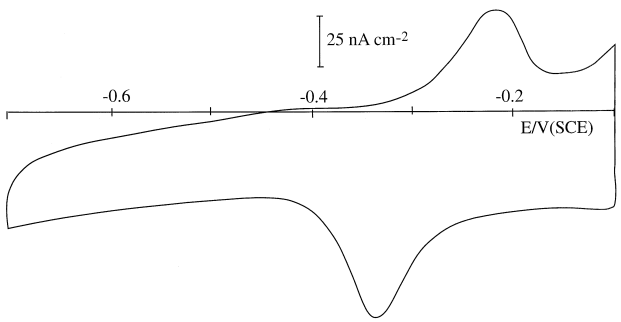

Fig. 1. Cyclic voltammogram of 1.5 mol% UQ in a supported DOPC monolayer in contact with a pH 9.5 solution of 0.1 M KCl + 0.01 M borate buffer. Scan rate $v = 5$ mV/s.

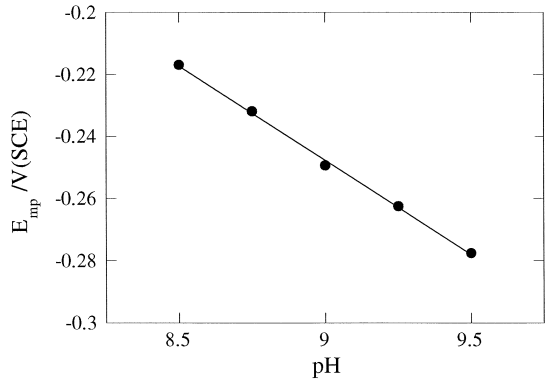

Fig. 2. Plot of the midpoint potential E_{mp} against pH as obtained from cyclic voltammograms of 1.5 mol% UQ in supported DOPC monolayers in contact with solutions of 0.1 M KCl + 0.01 M borate buffer of different pH values. Scan rate $v = 5$ mV/s.

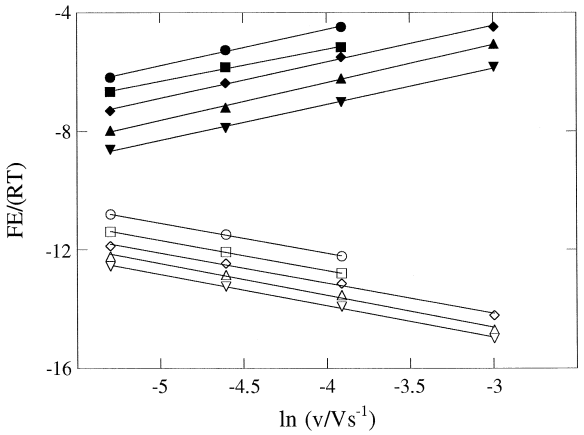

Fig. 3. Plots of $FE_{r,p}/(RT)$ vs. ln v (open symbols) and of $FE_{o,p}/(RT)$ vs. ln v (filled symbols) as obtained from cyclic voltammograms of 1.0 mol% UQ in supported DOPC monolayers in contact with solutions of 0.1 M KCl + 0.01 M borate buffer of different pH values: 8.5 (○, ●), 8.75 (□, ■), 9.00 (◇, ◆), 9.25 (△, ▲) and 9.50 (▽, ▼).

immersing a mercury drop through a layer of UQ spread on the surface of an aqueous electrolyte. The extrapolated value of the formal potential at pH 7, ≈ -0.13 V/SCE, is also in fairly good agreement with the value -0.15 V/SCE, determined by Takamiya and Dutton [20] from redox titrations of UQ in chromatophores, with the value -0.18 V/SCE, determined by Urban and Klingenberg [21] from mitochondrial preparations, or with the value -0.17 V/SCE, determined both by Rich [22] from model quinone behaviour in protic solvents and by Marchal et al. [7] from supported phospholipid layers.

An exceeding decrease in pH or increase in scan rate shifts the oxidation peak outside the region in which the lipid monolayer is impermeable to inorganic ions; when this occurs, the oxidation peak is notably obliterated by the high increase in capacitive current that accompanies the penetration of inorganic ions across the lipid film. Hence, no reliable measurements of the oxidation peak potential could be carried out at pH < 8.5 with a scan rate of 50 mV/s.

At the lower pH investigated (pH 8.5), repeated cycling does not affect the shape of cyclic voltammograms, provided that the scan rate v equals 5 mV/s. At higher scan rates, the time during which the electrode is maintained at potentials causing the reoxidation of UQH_2 to UQ along the positive potential scan is too short to allow a complete regeneration of UQ; hence, the reduction peak of UQ decreases somewhat in passing from the first to the subsequent cycles. In this case, the electrode was kept at an initial potential $E_{in} = -0.1$ V for a few seconds before the negative scan and only the first cyclic voltammogram was considered.

3.1. The reduction peak of UQ

Plotting the dimensionless quantity $FE_{r,p}/(RT)$ against ln v at constant pH, where v is the scan rate, yields a straight line of slope ≈ 1 over the whole pH

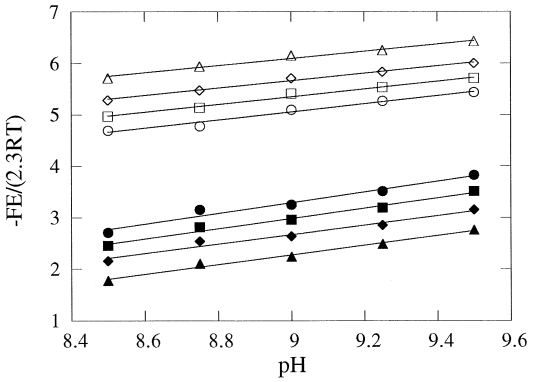

Fig. 4. Plots of $-FE_{r,p}/(2.3\ RT)$ vs. pH (open symbols) and of $-FE_{o,p}/(2.3\ RT)$ vs. pH (filled symbols) as obtained from cyclic voltammograms of 2.0 mol% UQ in supported DOPC monolayers in contact with solutions of 0.1 M KCl + 0.01 M borate buffer of different pH values. Scan rate: 5 (○, ●), 10 (□, ■), 20 (◇, ◆) and 50 (△, ▲) mV/s.

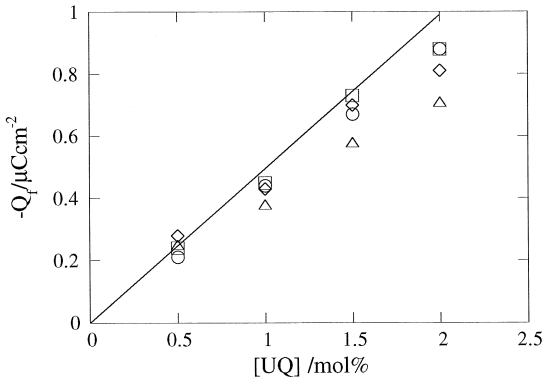

Fig. 5. Plots of the faradaic charge Q_f for UQ reduction against UQ concentration as obtained from cyclic voltammograms of UQ in supported DOPC monolayers in contact with pH 9.5 solutions of 0.1 M KCl + 0.01 M borate buffer at different scan rates: 5 (□), 10 (○), 20 (◇) and 50 (△) mV/s. The straight line was calculated for a complete two-electron reduction.

range investigated, as shown in Fig. 3. Plots of $-FE_{r,p}/(2.303\ RT)$ against pH at constant υ are also linear (Fig. 4), but their slope is somewhat less reproducible and ranges from ≈ 0.65 to ≈ 0.8. At any rate, a well-defined trend is always observed: an increase in the scan rate from 5 to 50 mV/s causes a moderate decrease both in the slope of the $-FE_{r,p}/(2.303\ RT)$ vs. pH plot and in the faradaic charge Q_f obtained upon integration of the area under the reduction peak. Fig. 5 shows plots of Q_f against the UQ concentration at different scan rates. The straight line in the same figure is the plot calculated for the case of a complete two-electron reduction of UQ to UQH_2 under the assumption that both the lipid and the UQ molecules occupy a surface area of 65 Å^2; incidentally, at the low UQ concentrations investigated, the uncertainty in the actual surface area occupied by one UQ molecule has an almost negligible effect on such an estimate. It is apparent that the experimental plot for $\upsilon = 5$ mV/s closely approaches the calculated straight line, at least for UQ concentrations < 2 mol%. However, a progressive increase in υ causes a gradual deviation from the straight line, which is larger the higher the UQ concentration is. Hence, increasing the scan rate and the UQ concentration prevents UQ from undergoing a complete reduction to UQH_2 along the reduction peak. These results agree with those obtained by the chronocoulometric technique [10], where deviations of Q_f from the calculated straight line are already observed at UQ concentrations > 0.5 mol% in view of the very short electrolysis time (50 ms) adopted with this technique.

Occasionally, the main reduction peak was followed by a smaller, more negative peak, as shown in

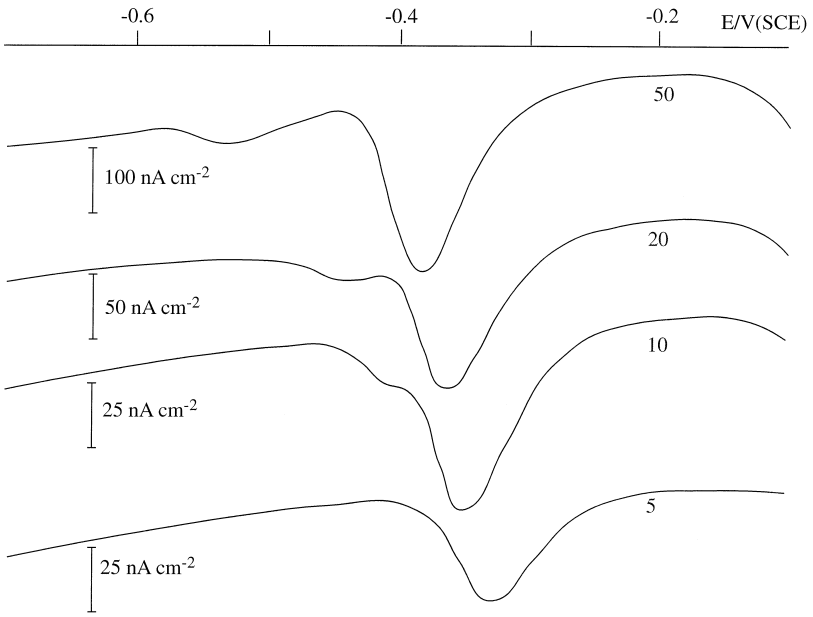

Fig. 6. Linear sweep voltammograms for the reduction of 1.5 mol% UQ in a supported DOPC monolayer in contact with a pH 9.5 solution of 0.1 M KCl + 0.01 M borate buffer. Numbers on each curve denote scan rates in mV/s.

the cyclic voltammograms of Fig. 6. At the lower scan rates, this further peak partially overlaps on the main one. An increase in scan rate causes the second peak to shift in the negative direction faster than the main one, until the two peaks are completely separated. Whenever the second peak overlapped partially on the main one, the background correction was first carried out by subtracting the cyclic voltammogram in the absence of UQ from that in its presence, under otherwise identical conditions; the graphical deconvolution program by Rakotondrainibe et al. [23] was then employed to estimate the peak potential, $E'_{r,p}$, of the second voltammetric peak. Plots of ln v vs. $FE'_{r,p}/(RT)$ have a slope of ≈ 0.5. $E'_{r,p}$ is practically independent of pH, at least over the narrow pH range investigated. The overall area under both reduction peaks decreases with an increase in v, similarly to what is observed in the presence of a single peak.

3.2. The oxidation peak of UQH_2

Plots of the dimensionless quantity $FE_{o,p}/(RT)$ against ln v at constant pH yield a straight line of slope ≈ 1 over the whole pH range investigated, as shown in Fig. 3. A practical unit slope is also exhibited by plots of $-FE_{o,p}/(2.303\ RT)$ against pH at constant v, for all scan rates investigated (see Fig. 4).

4. Discussion

To provide an interpretation of the experimental behaviour, an approach analogous to that already used in connection with the chronocoulometric technique [10] will be adopted. The deviations from the predictions of this approach will then be examined.

Briefly, the overall electrode reaction is regarded as consisting of a series of consecutive elementary electron-transfer and purely chemical steps; the chemical steps will be assumed to be protonation steps in UQ reduction and deprotonation steps in UQH_2 oxidation. Only one rate-determining step will be assumed, all other steps being in quasi-equilibrium. Under these conditions, a number of general approaches [10,24,25] leads to the following expression for the current density j:

$$\frac{j}{nF} = -\frac{d\Gamma_R}{dt} = kK\Gamma_R a_{H^+}^{\pm h} a_Y^y \exp\left[\mp(\vec{n}+\delta\alpha)\frac{FE}{RT}\right]. \quad (1)$$

Here and in the following, the upper sign refers to a reduction process and the lower sign to an oxidation process. F, R and T have their usual significance, whereas the meaning of the other symbols is as follows: E = applied potential; n = number of electrons involved in the overall electrode reaction; Γ_R = concentration of the reactant (UQ for the reduction, UQH_2 for the oxidation) in the lipid monolayer; $\vec{n}$ = number of electrons exchanged before the rate-determining step; k = rate constant for both the rate-determining step and the overall electrode reaction; K = overall equilibrium constant embodying the equilibrium constants of all protonation (or deprotonation) steps preceding the rate-determining step, as well as the exponential factors, $\exp(\pm FE^0_m/RT)$, for all $\vec{n}$ elementary electron-transfer steps preceding the rate-determining step, where E^0_m is the formal potential for the mth electron-transfer step; a_{H^+} = activity of hydrogen ions in the aqueous solution; h = number of elementary protonation steps (for the reduction) or deprotonation steps (for the oxidation) that precede the rate-determining step; a_Y = activity of the main proton donor (for the reduction) or of the main proton acceptor (for the oxidation) involved in the rate-determining step, if this is a protonation or a deprotonation step; y = molecularity of the rate-determining step with respect to the species Y (1 for a protonation or deprotonation rate-determining step, 0 for an electron-transfer rate-determining step); α = parameter equal to the symmetry factor $\beta \approx 1/2$ for the rate-determining uptake of one electron from the electrode, or to $(1-\beta)$ for the rate-determining release of one electron; δ = parameter equal to 1 for a rate-determining electron-transfer step, or to 0 for a rate-determining chemical step. Note that the potential dependence of the current in Eq. (1) has the same form as in the well-known Butler–Volmer equation.

In cyclic voltammetry, E is a linear function of time:

$$E = E_{in} \mp vt. \quad (2)$$

Here E_{in} is the initial potential and v is the absolute value of the scan rate; hence, the negative sign refers to a reductive scan while the positive sign refers to an oxidative scan. On substituting E from Eq. (2) into Eq. (1) and integrating the resulting equation over the electrolysis time t from $t=0$ to $t=t$ by separation of variables, we get:

$$\int_{\Gamma_R(t)}^{\Gamma_R(0)} \frac{d\Gamma_R}{\Gamma_R} = \text{const}\frac{a_{H^+}^{\pm h} a_Y^y}{v}\exp\left[(\vec{n}+\delta\alpha)\frac{F(vt \mp E_{in})}{RT}\right] = \text{const}\frac{a_{H^+}^{\pm h} a_Y^y}{v}\exp\left[\mp(\vec{n}+\delta\alpha)\frac{FE}{RT}\right] \quad (3)$$

where:

$$\text{const} = \frac{RT}{(\vec{n}+\delta\alpha)F}kK. \quad (4)$$

Here $\Gamma_R(0)$ and $\Gamma_R(t)$ are the concentrations of the reactant R before the electrolysis and at time t, respectively. In integrating Eq. (1) to yield the second member of Eq. (3), unity was neglected with the respect to the exponential factor; this neglect is entirely justified provided that the initial potential E_{in} precedes the voltammetric peak by no less than about 100 mV.

By definition, the faradaic charge $Q_f(t)$ that consumes the reactant R is given by:

$$Q_f(t) = \int_0^t j(t)dt = -nF\int_0^t \frac{d\Gamma_R}{dt}dt = nF[\Gamma_R(0) - \Gamma_R(t)] \quad (5)$$

and hence a constant value of $Q_f(t)$ implies a constant value of $\Gamma_R(t)$. By keeping constant both $Q_f(t)$ and the initial concentration of R (i.e., $\Gamma_R(0)$) the first member in Eq. (3) is therefore constant, and the same is true for the third member. Under these conditions, differentiation of the logarithm of the latter member with respect to E at constant pH and with respect to pH at constant v yields:

$$\frac{RT}{F}\left(\frac{\partial \ln v}{\partial E}\right)_{pH,Q_f,\Gamma_R(0)} = \mp(\vec{n}+\delta\alpha) \quad (6)$$

and

$$\frac{F}{2.3\,RT}\left(\frac{\partial E}{\partial pH}\right)_{v,Q_f,\Gamma_R(0)} = \frac{-h \pm y(\partial \log a_y/\partial pH)}{(\vec{n}+\delta\alpha)}. \quad (7)$$

The left-hand sides of Eqs. (6) and (7) were estimated by measuring how the potential corresponding to a constant faradaic charge Q_f varies with the logarithm of the scan rate v at constant pH, or else with pH at constant v. These measurements were carried out for a constant initial concentration of UQ in the lipid monolayer; naturally, when carrying out oxidative potential scans, the initial concentration was that of UQH_2 resulting from the previous total reduction of UQ in the lipid film.

As a rule, for a constant initial concentration of UQ, the faradaic charge Q_f obtained by integrating the area under the voltammetric reduction or oxidation peak from its onset up to the peak potential $E_{r,p}$ or $E_{o,p}$ was found to remain substantially constant when varying the scan rate or the pH. Hence, the rates of change of $E_{r,p}$ or $E_{o,p}$ with varying ln v at constant pH and with varying pH at constant v were directly employed in Eqs. (6) and (7). In those cases in which the charge under the voltammetric peaks for UQ reduction was found to decrease appreciably with an increase in scan rate, the potentials at constant faradaic charge were estimated by integrating the area under the various reduction peaks from their onset up to attainment of a faradaic charge Q_f equal to that corresponding to the peak potential $E_{r,p}$ for the reduction peak recorded at the lowest scan rate. As the scan rate is increased, the potentials at constant Q_f so-obtained shift progressively, albeit very slightly, in the negative direction with respect to the corresponding peak potentials. In practice, however, this correction is so small that it hardly affects the slopes of the resulting plots of $FE/(RT)$ at constant Q_f vs. ln v or vs. pH with respect to the corresponding plots of $FE_{r,p}/(RT)$ vs. ln v or vs. pH.

The plots of $FE_{o,p}/(RT)$ vs. ln v for the oxidation of 1.0 mol% UQH_2 at different pH values over the v range from 5 to 50 mV/s (see Fig. 3) are linear and exhibit slopes that are practically equal to unity at all pH values investigated. The plots of $-FE_{o,p}/(2.3\,RT)$ vs. pH in Fig. 4 are also approximately linear and exhibit a unit slope. In view of Eq. (6), the unit

slope of the experimental $FE_{o,p}/(RT)$ vs. ln υ plots indicates that the quantity $(\vec{n}+\delta\alpha)$ is also equal to unity. Since α is expected to be close to $1/2$, it must be concluded that $\vec{n}=1$ and $\delta=0$, and hence, that the rate-determining step is a deprotonation step following the reversible release of the first transferring electron. This conclusion is supported by the slope of the $-FE_{o,p}/(2.3\ RT)$ vs. pH plot being approximately equal to unity. In fact, this slope can be justified on the basis of Eq. (7) by setting $h=0$, $y=1$ and by identifying the main proton acceptor Y with the hydroxyl ion, which implies that $(\partial\log a_Y/\partial\mathrm{pH})$ is also equal to unity. The resulting reaction mechanism is:

$$\mathrm{UQH_2}-e^-\leftrightarrow\mathrm{UQH_2^{+\cdot}};\mathrm{UQH_2^{+\cdot}}+\mathrm{OH^-}\overset{\text{rds}}{\rightarrow}\mathrm{UQH^{\cdot}}+\mathrm{H_2O};\mathrm{UQH^{\cdot}}+\mathrm{OH^-}-e^-\leftrightarrow\mathrm{UQ}+\mathrm{H_2O}. \quad (8)$$

The plots of $FE_{r,p}/(RT)$ vs. ln υ for the reduction of 1.0 mol% UQ at different pH values over the υ range from 5 to 50 m V/s (see Fig. 3) are linear and exhibit slopes approximately equal to unity at all pH values investigated. The plots of $-FE_{r,p}/(2.3\ RT)$ vs. pH in Fig. 4 are also approximately linear; however, they exhibit slopes less than unity that decrease slightly with an increase in scan rate. Within the limits in which the deviations of the latter plots from unity can be disregarded, considerations entirely analogous to those made in connection with $\mathrm{UQH_2}$ oxidation lead to the conclusion that the rate-determining step for UQ reduction is the protonation of the radical anion $\mathrm{UQ^{\cdot-}}$ involving the proton as the only effective proton donor, according to the mechanism:

$$\mathrm{UQ}+e^-\leftrightarrow\mathrm{UQ^{-\cdot}};\mathrm{UQ^{-\cdot}}+\mathrm{H^+}\overset{\text{rds}}{\rightarrow}\mathrm{UQH^{\cdot}};\mathrm{UQH^{\cdot}}+\mathrm{H^+}+e^-\leftrightarrow\mathrm{UQH_2}. \quad (9)$$

In principle, plots of $-FE/(2.3\ RT)$ vs. pH for UQ reduction carried out by the chronocoulometric technique at constant Q_f and electrolysis time t should exhibit slopes identical with those of plots of $-FE_{r,p}/(2.3\ RT)$ vs. pH carried out by the voltammetric technique. Plots of $-FE/(2.3\ RT)$ vs. pH obtained in Ref. [10] by chronocoulometry show indeed slopes of ≈ 0.8. In that paper, these deviations from the expected unit value were ascribed to Langmuirian adsorption of protons in the polar-head region. The long time-scale voltammetric behaviour reported herein brings to light further interesting features: thus, a gradual increase in scan rate causes a progressive decrease both in the slope of $-FE_{r,p}/(2.3\ RT)$ vs. pH plots and in the charge associated with the reduction peak of UQ. This correlation between decrease in charge and decrease in pH dependence is shown in Fig. 7. This strongly suggests that the decrease in the pH dependence of UQ reduction is due to an incomplete reduction of the intermediate semiubiquinone radical anion, $\mathrm{UQ^{\cdot-}}$, during the recording of the UQ voltammetric peak. The higher the scan rate, the larger the amount of $\mathrm{UQ^{\cdot-}}$ that remains in the lipid film at the end of the voltammetric peak, and hence, the smaller the charge associated with this peak. This phenomenon must also be accompanied by a decrease in the pH dependence of UQ reduction; in fact, this dependence stems from the rate-determining protonation of the semiubiquinone radical anion, which is followed by the almost instantaneous reduction of the resulting neutral radical $\mathrm{UQH^{\cdot}}$ to ubiquinol.

To provide a semiquantitative explanation of the above experimental behaviour, alternative mechanisms were examined. One mechanism postulates a

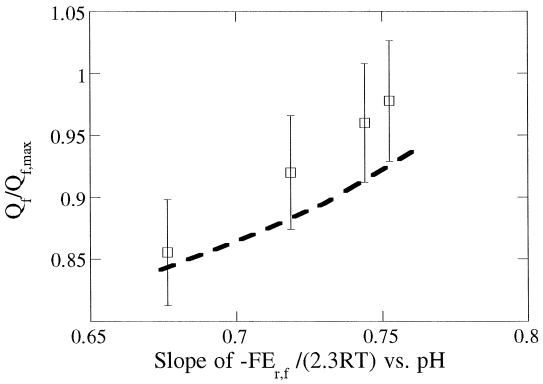

Fig. 7. Plot of the faradaic charge for UQ reduction against the pH dependence of its kinetics. The faradaic charge is expressed by the $Q_f/Q_{f,max}$ ratio, where Q_f is the experimental faradaic charge associated with the reduction peak of UQ and $Q_{f,max}$ is the faradaic charge calculated for a complete two-electron reduction. The pH dependence is expressed by the slope of the $-FE_{r,p}/(2.3\ RT)$ vs. pH plot. The dashed curve was calculated according to mechanism A for $r=0.8$, $m_0\equiv RTk_0/(F\upsilon)$ varying from 7 to 0.7 to allow for the change in the scan rate υ, and $\vartheta\equiv k_0/k_p=k_0/(k'_p[\mathrm{H^+}])$ varying from 5 to 0.5 to allow for the change in pH.

single type of reaction site for the reduction of the electroactive moiety of the UQ molecule; here UQ undergoes a 'quasi-reversible' electron-transfer step, namely a step whose backward rate is not entirely negligible with respect to the forward one. The resulting semiubiquinone radical anion undergoes a protonation step, which is allowed to proceed at a lower rate, thus causing an accumulation of $UQ^{\cdot -}$. The protonated semiubiquinone radical, $UQH^{\cdot}$, undergoes an instantaneous electroreduction to ubiquinol. Linear potential sweep voltammograms for the above mechanism were calculated by the appropriate modification of Laviron's treatment for a quasi-reversible electron transfer without diffusion [26]. This mechanism cannot account for the experimental behaviour. Thus, no pair of values of the standard rate constant k_0 for the electron-transfer step and of the protonation rate constant k_p can justify simultaneously a unit slope for the $FE_{r,p}/(RT)$ vs. ln υ plot and a slope of $0.65 \div 0.8$ for the $-FE_{r,p}/(2.3\ RT)$ vs. pH plot. Moreover, at the high k_p values required to predict the relatively large experimental pH dependence of UQ reduction, the $UQ^{\cdot -}$ concentration extremely low along the whole voltammetric peak, with the result that the calculated charge associated with this peak amounts constantly to 2 Faradays per mole of UQ.

A further mechanism (mechanism A) postulates two types of reaction sites for UQ reduction. The first site is readily accessible to protons, which allows the electron-transfer step and the subsequent protonation step to proceed under steady-state conditions with complete reduction of UQ to UQH_2. Conversely, the second site is inaccessible to protons in the time scale of the cyclic-voltammetric measurements, causing UQ reduction to stop after the first electron-transfer step. Nonetheless, the UQ and $UQ^{\cdot -}$ molecules are allowed to partition freely between the two reaction sites; with this assumption a single voltammetric peak is again predicted. Details of this mechanism are outlined in Appendix A. The standard rate constant k_0 for the electron-transfer step is assumed to be the same at both sites. Mechanism A accounts satisfactorily for the experimental behaviour of the single voltammetric peak that is usually observed in UQ reduction. Thus, for suitable values of k_0 and k_p it predicts an approximately unit slope of the $FE_{r,p}/(RT)$ vs. ln υ plot. It also predicts a gradual decrease both in the slope of the $-FE_{r,p}/(2.3\ RT)$ vs. pH plot and in the faradaic charge Q_f associated with the voltammetric peak as the scan rate is progressively increased. The dashed curve of Q_f against the slope of the $-FE_{r,p}/(2.3\ RT)$ vs. pH plot in Fig. 7 was calculated according to this mechanism. Quite probably, the reaction site inaccessible to protons is located deeper inside the lipid monolayer with respect to that accessible to protons.

The occasional appearance of two distinct peaks for UQ reduction can only be explained by assuming the presence of a 'UQ-rich' phase that is not constrained by the ordered chains of the membrane lipid: the UQ molecules are practically segregated into these UQ-rich pockets and cannot exchange freely with the UQ molecules intercalated in the lipid monolayer, at least in the time scale of cyclic voltammetric measurements. The possibility that the slowly protonating quinone radical pool may be directly adsorbed on the electrode surface cannot be excluded. With respect to the aqueous phase, such a position is equivalent to that in the midplane of a lipid bilayer: the latter position was postulated by several researchers [27–31]. The presence of the second voltammetric peak in Fig. 6 can be ascribed to a reduction of the UQ molecules trapped in these UQ-rich pockets under the control of the first electron-transfer step. Thus, the slope of the ln υ vs. $FE'_{r,p}/(RT)$ plot relative to the second peak yields a value of ≈ 0.5 for the quantity $(\vec{n} + \delta\alpha)$, in view of Eq. (6); this can be readily interpreted by setting $\vec{n} = 0$ and $\delta = 1$, namely by assuming that UQ reduction is controlled by the uptake of the first transferring electron. Moreover, the pH-independence of the second peak excludes a protonation step in quasi-equilibrium preceding the rds. Fig. 8 shows cyclic voltammograms calculated by ascribing the first peak to UQ reduction according to mechanism A and the second peak to the irreversible reduction of UQ molecules trapped in the UQ-rich pockets.

The necessity of passing the mercury drop a few times across the (DOPC + UQ) layer over the range of UQ concentrations from 0.5 to 2 mol% in order to transfer on the mercury drop a lipid monolayer with the same features as those of a pure monolayer may indeed be ascribed to the tendency of the UQ molecules to segregate: repeated immersions may favour the intercalation of these molecules in the

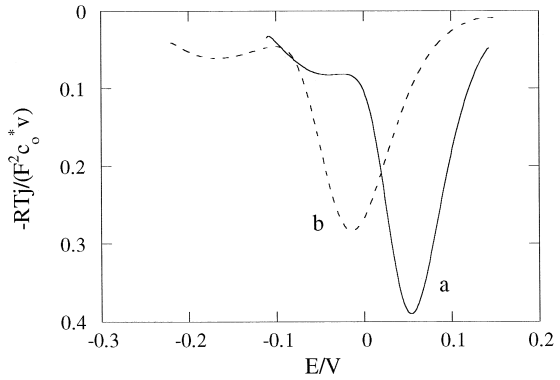

Fig. 8. Linear sweep voltammograms for UQ reduction calculated by setting the fraction of intercalated UQ molecules to those in the UQ-rich phase equal to 0.6. The more positive peak was calculated on the basis of mechanism A from Eqs. (5A) and (6A) for $r = 0.8$, $\vartheta = 0.5$ and $\beta = 0.5$, whereas the more negative one was calculated from Eq. (8A) for $\beta' = 0.4$. Curve *a* was obtained for $m_0 = 7$ and $m'_0 = 0.3$, whereas curve *b* was obtained for $m_0 = 0.7$ and $m'_0 = 3\times10^{-2}$ in order to increase the scan rate v by one order of magnitude.

lipid monolayer. The existence of two distinct UQ phases, suggested by the cyclic voltammograms in Fig. 6, with a slow exchange between their populations, was also proposed on the basis on a ^{1}H-NMR investigation of UQ in perdeutarated PC bilayers [32]. It is apparent that the higher local concentration of UQ in the UQ-rich phase affects the kinetic properties of UQ and stabilizes the $UQ^{\cdot-}$ radical anion. The lifetime of the radical anion is appreciable even when a single voltammetric peak is observed, as indicated by the concomitant decrease in its pH dependence and in the corresponding faradaic charge with an increase in scan rate (see Fig. 7). This may have some implications for the function of UQ in biological membranes such as the inner mitochondrial membrane or the photosynthetic vesicle of purple bacteria, where the secondary acceptor Q_B is considered to accept two electrons, one after the other, before undergoing protonation.

Acknowledgements

The authors wish to thank Mr. Luciano Righeschi for valuable technical assistance. Thanks are due to the Ministerio de Educación y Cultura, Spain, for the fellowship to R.H., during the tenure of which the present results were obtained. The financial support of the Ministero dell'Universita' e della Ricerca Scientifica e Tecnologica and of the Consiglio Nazionale delle Ricerche is gratefully acknowledged.

Appendix A

Let us consider the reaction mechanism:

$$O + e^- \overset{k_0}{\leftrightarrow} R \overset{k_p}{\leftrightarrow} O_1 + e^- \Leftrightarrow R_1 \qquad (1A)$$

where the first electron-transfer step yields an intermediate reduction product R that undergoes an irreversible chemical step, with rate constant k_p. As soon as it is formed, the product O_1 of this chemical step is instantaneously reduced to the final product R_1. Let k_0 denote the standard rate constant of the first electron-transfer step, regarded as quasi-reversible. When applying this scheme to UQ reduction, the symbols O, R, O_1 denote UQ, $UQ^{\cdot-}$, $UQH^{\cdot}$ and UQH_2, and the rate constant $k_p \equiv k'_p[H^+]$ embodies the hydrogen ion concentration. According to mechanism A, at the reaction sites accessible to protons (briefly denoted by a-sites) the process of Eq. (1A) takes place under steady-state conditions, whereas at the reaction sites inaccessible to protons (b-sites) it stops at the intermediate product R. The rate of the process at the a-sites, v_a, is therefore equal to the common value of the rate of the first electron-transfer step and of the subsequent chemical step:

$$v_a = k_0\left(c_O\eta^{-\beta} - c_R\eta^{1-\beta}\right) = k_p C_R \rightarrow v_a = \frac{k_p k_0 c_O \eta^{-\beta}}{k_p + k_0\eta^{1-\beta}}. \qquad (2A)$$

Here the rate of the first electron-transfer step is expressed by the well-known Butler–Volmer equation, where β is the symmetry factor, η is defined by:

$$\eta \equiv \exp\left[\frac{F(E - E_0)}{RT}\right]$$

and E_0 is the formal potential of the O/R couple; c_O and c_R are the concentrations of O and R in the lipid film. The rate v_b at b-sites is simply expressed by the Butler–Volmer equation:

$$v_b = k_0\left(c_O\eta^{-\beta} - c_R\eta^{1-\beta}\right). \qquad (3A)$$

Denoting by r the ratio of the number of a-sites to the total number of sites in the lipid monolayer, we have:

$$-\frac{dc_O}{dt} = rv_a + (1-r)v_b \text{ (a)};$$

$$-\frac{dc_R}{dt} = rv_a - (1-r)v_b \text{ (b)}. \quad (4A)$$

These two equations account for the instantaneous partition of both O and R between a- and b-sites. Upon denoting by c_O* the concentration of O before electrolysis, let us introduce the following dimensionless quantities:

$$\rho_O \equiv \frac{c_O}{c_O*}; \rho_R \equiv \frac{c_R}{c_O*}; m_0 \equiv \frac{RT}{F}\frac{k_0}{v}.$$

Taking into account that during a reductive potential scan, we have $dt = -dE/v$ (see Eq. (2)), Eqs. (2A), (3A) and (4A) take the form:

$$\frac{d\rho_O}{dE} = \frac{F}{RT}\left[\frac{rm_0\rho_O\eta^{-\beta}}{1+\vartheta\eta^{1-\beta}} + (1-r)m_0 \times\left(\rho_O\eta^{-\beta} - \rho_R\eta^{1-\beta}\right)\right] \quad (5A)$$

$$\frac{d\rho_R}{dE} = \frac{F}{RT}\left[\frac{rm_0\rho_R}{\vartheta} + (1-r)m_0 \times\left(\rho_R\eta^{1-\beta} - \rho_O\eta^{-\beta}\right)\right]$$

$$\text{with } \vartheta \equiv \frac{k_0}{k_p} = \frac{k_0}{k'_p[H^+]}. \quad (6A)$$

The disappearance of 1 mole of O contributes 2 Faradays to the charge density, provided that we subtract 1 Faraday for each mole of R that is formed in place of the final reduction product R_1. Hence, the current density is given by:

$$j = -2F\frac{dc_O}{dt} - F\frac{dc_R}{dt} = Fc_O*v\left(2\frac{d\rho_O}{dE} + \frac{d\rho_R}{dE}\right). \quad (7A)$$

The voltammograms relative to mechanism A can be calculated by integrating the two differential Eqs. (5A) and (6A) over E by the fourth-order Runge–Kutta method, with the initial conditions $\rho_O = 1$ and $\rho_R = 0$.

In the presence of a pool of UQ molecules that do not exchange with the molecules intercalated in the lipid monolayer, the overall current density is just the sum of the current density expressed by Eq. (7A) due to the intercalated UQ molecules, and of a current density due to the quasi-reversible or irreversible reduction of the UQ molecules of the pool. The latter current is calculated by solving the differential equations:

$$\frac{d\rho'_O}{dE} = \frac{F}{RT}m'_0\left(\rho'_O\eta^{-\beta'} - \rho'_R\eta^{1-\beta'}\right);$$

$$\frac{d\rho'_R}{dE} = \frac{F}{RT}m'_0\left(\rho'_R\eta^{1-\beta'} - \rho'_O\eta^{-\beta'}\right) \quad (8A)$$

where the dimensionless concentrations ρ'_O, ρ'_R, the dimensionless standard rate constant m'_0 and the symmetry factor β' are generally different from those for the intercalated UQ molecules.

References

[1] G. Cauquis, G. Marbach, Biochim. Biophys. Acta 283 (1972) 239–246.
[2] J.Q. Chambers, in: S. Patai (Ed.), The Chemistry of the Quinonoid Compounds, Wiley, New York, 1974, pp. 737–791.
[3] R.C. Prince, P.L. Dutton, J.M. Bruce, FEBS Lett. 160 (1983) 273–276.
[4] K. Takehara, H. Takemura, Y. Ide, S. Okayama, J. Electroanal. Chem. 308 (1991) 345–350.
[5] J.M. Laval, M. Majda, Thin Solid Films 244 (1994) 836–840.
[6] S. Sanchez, A. Arratia, R. Cordova, H. Gomez, R. Schrebler, Bioelectrochem. Bioenerg. 36 (1995) 67–71.
[7] D. Marchal, W. Boireau, J.M. Laval, J. Moiroux, C. Bourdillon, Biophys. J. 72 (1997) 2679–2687.
[8] M.A. Stidham, T.J. McIntosh, J.N. Siedow, Biochim. Biophys. Acta 767 (1984) 423–431.
[9] P.R. Rich, R. Harper, FEBS Lett. 269 (1990) 139–144.
[10] M.R. Moncelli, L. Becucci, A. Nelson, R. Guidelli, Biophys. J. 70 (1996) 2716–2726.
[11] A. Nelson, A. Benton, J. Electroanal. Chem. 202 (1986) 253–270.
[12] M.R. Moncelli, L. Becucci, R. Guidelli, Biophys. J. 66 (1994) 1969–1980.
[13] M.R. Moncelli, L. Becucci, J. Electroanal. Chem. 385 (1995) 183–189.

[14] M.R. Moncelli, L. Becucci, J. Electroanal. Chem. 443 (1997) 91–96.
[15] M.R. Moncelli, L. Becucci, R. Herrero, R. Guidelli, J. Phys. Chem. 99 (1995) 9940–9951.
[16] M.L. Foresti, M.R. Moncelli, R. Guidelli, J. Electroanal. Chem. 109 (1980) 1–14.
[17] L. Becucci, M.R. Moncelli, R. Guidelli, J. Electroanal. Chem. 413 (1996) 187–193.
[18] I.R. Miller, in: G. Milazzo (Ed.), Topics in Bioelectrochemistry and Bioenergetics, Wiley, Chichester, 1981, pp. 194–225.
[19] G.J. Gordillo, D.J. Schiffrin, J. Chem. Soc. Faraday Trans. 90 (1994) 1913–1922.
[20] K.-I. Takamiya, P.L. Dutton, Biochim. Biophys. Acta 546 (1979) 1–16.
[21] P.F. Urban, M. Klingenberg, Eur. J. Biochem. 9 (1969) 519–525.
[22] P.R. Rich, Biochim. Biophys. Acta 768 (1984) 53–79.
[23] A. Rakotondrainibe, B. Beden, C. Lamy, J. Electroanal. Chem. 379 (1994) 455–465.
[24] J.O'M. Bockris, A.K.N. Reddy, Modern Electrochemistry, Vol. 2, Plenum, New York, 1970, pp. 997–1002.
[25] H. Mauser, Z. Elektrochem. Ber. Bunsenges. Physik. Chem. 62 (1958) 419–425.
[26] E. Laviron, J. Electroanal. Chem. 101 (1979) 19–28.
[27] P.J. Quinn, M.A. Esfahani, Biochem. J. 185 (1980) 715–722.
[28] H. Katsikas, P.J. Quinn, Biochim. Biophys. Acta 689 (1982) 363–369.
[29] M. Ondarroa, P.J. Quinn, Eur. J. Biochem. 155 (1986) 353–361.
[30] E.L. Ulrich, M.E. Girvin, W.A. Cramer, J.L. Markley, Biochemistry 24 (1984) 2501–2508.
[31] B.A. Cornell, M.A. Keniry, A. Post, R.N. Robertson, L.E. Weir, P.W. Westerman, Biochemistry 26 (1987) 7702–7707.
[32] P.B. Kingsley, G.W. Feigenson, Biochim. Biophys. Acta 635 (1981) 602–618.